TOWARDS A MORE FLEXIBLE RATING METHOD FOR CABLES IN TUNNELS

J. A. Pilgrim*, D. J. Swaffield*, P. L. Lewin*, S. T. Larsen and D. Payne*****

***University of Southampton, UK **Southampton Dielectric Consultants, UK ***National Grid, UK**

ABSTRACT

In recent years the use of cable tunnels in large urban areas has become more popular, with the additional capital cost becoming increasingly acceptable in light of the growing difficulties incurred for large scale directly buried cable installations. Presently cable ratings for such circuits are calculated using the method of Electra 143. However the applicability of this method is restricted owing to the assumptions made within the calculation, notably that all cables must be of identical construction and carrying equal load. This work demonstrates an improved method which removes this limitation whilst retaining the ease of use of the previous method.

INTRODUCTION

Cable tunnels first came into significant use during the construction of the 400kV supergrid in the 1960's, where it became necessary to use tunnels to carry transmission circuits under bodies of water, for instance beneath Southampton Water at Fawley and the River Thames in London [1]. The popularity of tunnels has increased as network reinforcements have become required in London, for instance the new Dartford cable tunnel and the 20km long Elstree – St Johns Wood tunnel [2]. The use of cable tunnels is not just limited to transmission, with a number of tunnels now housing distribution cables within central London [3]. With a number of schemes currently under construction or under consideration, the quantity of cable installed within tunnels is set to increase. Due to the magnitude of capital investment required to build cable tunnels, it is essential that the current rating of the cables can be found accurately. This paper examines the present rating method for force ventilated cable tunnels and develops an improved method specifically to rate cases of multiple cable circuits within a single tunnel.

Present Method

The numerical method of Electra 143 is the most commonly used method for calculating the ratings of cables installed in force ventilated cable tunnels [4]. It allows the calculation of both steady state and transient temperature distributions based on a lumped parameter thermal – electrical analogue approach. A 1D thermal network is created to represent a slice through the tunnel cross section, with a number of these meshes being connected axially to represent the full length of the tunnel.

A number of assumptions are necessary for the method to function correctly. Air flow within the tunnel must be sufficiently high for turbulent flow to occur, with the cables laid in direct contact with the air. The tunnel cross-section must also be constant throughout the length of the route. Perhaps the most important assumption is that regarding the cables themselves. Each cable must be of identical construction, operate at the same voltage and carry the same current. Applying this restriction reduces the complexity of the thermal network as it is only necessary to directly model one cable. In reality such a condition is rarely achieved, with the obvious exception of a tunnel containing a single cable circuit.

Issues Indentified

This restriction on the modelling of the cable is one of the key failings of the Electra method and can become particularly inconvenient in cases where circuits of multiple voltage levels are installed within one tunnel. A further issue is the lack of consideration for the thermal conditions of the cable within the riser shafts. Depending on the depth of these shafts and the ventilation conditions, it is possible that the core temperature of the cable installed here could pose a limiting factor to the overall circuit rating. Additionally no direct consideration is given to the thermal effects of cable joints within the system.

Method Requirements

The method discussed in the remainder of this paper is intended to remove the limitation of identical cables in order to increase the flexibility of the calculation procedure. The Electra method is reasonably quick to build and to solve, a feature which must be retained for the new method to be of operational benefit. The lumped parameter approach can deliver both of these requirements as is demonstrated in the following section.

MODEL CONSTRUCTION

Construction of the thermal network is largely similar to that of Electra 143, however to allow for dissimilar cables a number of modifications are necessary.

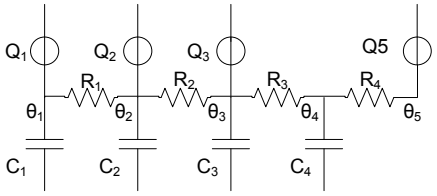

Figure 1 – Equivalent thermal network of cable

$$R_1 = R_2 = \frac{\rho_t}{4\pi\Delta x}\ln\left(1+\frac{2t_1}{d_c}\right) \quad (1)$$

$$R_3 = R_4 = \frac{\rho_s}{4\pi\Delta x}\ln\left(\frac{D_e}{D_s}\right) \quad (2)$$

$$C_1 = A_c c_{pc}\Delta x \quad (3)$$

$$C_2 = \frac{\pi}{4}\left[(d_c+2t_1)^2 - {d_c}^2\right]c_{pt}\Delta x \quad (4)$$

$$C_3 = \frac{\pi}{4}\left[D_s^2 - (d_c+2t_1)^2\right]c_{pm}\Delta x \quad (5)$$

$$C_4 = \frac{\pi}{4}\left[D_e^2 - D_s^2\right]c_{ps}\Delta x \quad (6)$$

$$Q_1 = I^2 R_{ac}\Delta x \quad (7)$$

$$Q_2 = 2\pi f C_d U^2 \tan\delta \quad (8)$$

$$Q_3 = \lambda I^2 R_{ac}\Delta x \quad (9)$$

Cable Representation

Each cable can be represented by five nodal points, connected by the thermal resistances specified in (1) and (2). The locations of these nodes are as specified in [4], i.e.

1. Conductor (which is assumed isothermal)
2. Log mean value of dielectric
3. Centre of cable sheath (which is assumed isothermal)
4. Log mean radius of the serving
5. Outer surface of cable

Nodes internal to the cable have a thermal capacitance associated with them (3)-(6), along with heat sources due to joule, dielectric and sheath losses (7)-(9) at nodes one, two and three respectively. The equivalent circuit for the cable can be seen in Fig 1. The lumped parameter model of the cable circuit has been compared to a steady state FEA cable model to verify its accuracy. Agreement between the two models was observed to be within 0.1°C for both the conductor and surface temperatures.

Tunnel Representation

Whilst the representation of the cable is largely common with Electra 143, a significant modification to the modelling of the tunnel environment is required. To allow the individual cables to have independent load cycles and construction, the sum of the convective

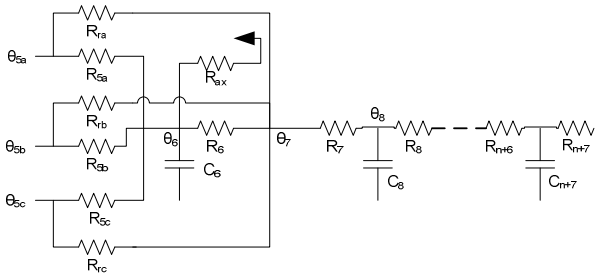

Figure 2 – Equivalent thermal network of tunnel

and radiation heat transfer must be considered at nodes 6 (representing the tunnel air) and 7 (representing the tunnel wall) respectively. The equivalent thermal network for the case of one circuit is shown in Fig 2. The left hand side of Fig. 2 shows the connection to node 5 at the outer edge of the cable. The method does not pose a limit on the number of independent cables for which a temperature distribution can be obtained.

Tunnel Air Thermal elements connecting the cable surface (nodes 5a onwards in Fig. 2) to the tunnel air (node 6) are calculated by (10). The thermal resistance between the tunnel air and the tunnel wall can be calculated by (11), with the thermal capacitance of the tunnel air itself defined by (12).

$$R_5 = \frac{1}{\pi D_e h_{cab}\Delta x} \quad (10)$$

$$R_6 = \frac{1}{\pi D_{tun} h_{wall}\Delta x} \quad (11)$$

$$C_6 = c_{pf} A_f \Delta x \quad (12)$$

Calculation of the cable and tunnel wall convective heat transfer coefficients will depend on the velocity of the air within the tunnel. The method described in Electra 143 suggests the work of Weedy and El-Zayyat [5] should be used to find h_{cab} and the standard Dittus-Boelter correlation for h_{wall} [6]. An additional thermal resistance is required to account for the connection between individual slices (that shown as R_{ax} in Fig. 2). This resistance (13) links node 6 of each slice to that of the preceding slice, or to the air inlet temperature in the case of the first slice.

$$R_{ax} = \frac{1}{c_{pf} V A_f} \quad (13)$$

Tunnel Walls Heat is transferred to the tunnel walls by both convection (according to (11)) and radiation. This requires an extra resistance element from each cable surface to the wall (node 7), calculated by (14).

Heat Transfer Between Cables Where more than one circuit is installed within a tunnel, and operating under different load cycles, the cable surface temperatures will not match. As a result, radiation heat transfer can occur between cables, as well as between the cable and the wall. This can be accounted for by considering an additional heat source (15) at each cable surface receiving heat (or an additional heat sink for those

$$Rr = \frac{1}{\sigma F_{cw} D_e \varepsilon_{cab} \Delta x \left((\theta_5 + 273.15)^2 + (\theta_7 + 273.15)^2 \right)} \frac{1}{(\theta_5 + 273.15) + (\theta_7 + 273.15)} \tag{14}$$

$$Q_{5,y} = \pi D_e \Delta x \varepsilon_{cab} \sigma \sum_{c=1}^{N} F_{cc(y,c)} \left((\theta_{5(y)} + 273.15)^4 - (\theta_{5(c)} + 273.15)^4 \right) \tag{15}$$

cables with a net loss of heat energy to other cables, represented by Q_5 in Fig. 1). Note that y denotes the cable under consideration and $F_{cc(y,c)}$ is the view factor between cables y and c. Values for view factors between cables can be calculated in a number of ways. The simplest method is that of crossed strings, as described in [7], which can be solved by a simple algebraic equation where the cable diameters are approximately equal. For more complex geometries, a contour integral solution may be necessary [8]. The view factor F_{cw} can then be found easily using (16).

$$F_{cw(y)} = 1 - \sum_{c=1}^{N} F_{cc(c,y)} \tag{16}$$

Surrounding Soil The heat transfer within the medium surrounding the tunnel may be solved using the method outlined in Electra 143. This requires the region to be split into annular rings, with a thermal resistance and capacitance assigned to each. It is recommended that the node locations be calculated using the power law expression stated in Electra 143 [4].

SOLUTION PROCEDURE

Under the scheme laid out in Electra 143, it is possible to solve the entire system using one set of matrices where the equations are re-arranged into tridiagonal matrix form. However, where more than one cable mesh is present at each axial slice through the tunnel, this is no longer possible. Instead it is proposed that the calculation is separated into two components which are iterated sequentially. The first calculation requires the solution of an array of matrices containing the first five nodal equations representing the cables. Results from this calculation are then fed into a second matrix system containing all the nodal equations for the tunnel environment.

Cable System Equations To correctly represent the cables within the tunnel, equations (17) – (21) must be solved for each individual cable. It should be noted that the superscript m within these equations represents the present timestep or iteration. Hence m+1 denotes the new values of nodal temperature found by solving the equation set and m=1 would represent the initial conditions. For each calculation the most recent values of nodal temperatures are used. Referring to equations (14-15), it is clear that these equations must be updated prior to each iteration as they both depend on the nodal temperatures at the cable surface and at the tunnel wall.

Tunnel Environment Equations Having solved for the temperature distribution within each cable, the tunnel environment temperatures must be recalculated. Prior to doing so, the values of equations (14) and (15) must again be updated with the new values of cable surface temperature (node 5). The necessary equations are those shown in (22) – (24). Equation (24) represents the generic form of the relation used to solve for nodal temperatures in the medium surrounding the tunnel. The cable system equations are then resolved using the new values of tunnel air and tunnel wall temperature to obtain the temperature profile for the given iteration.

Steady State

For the steady state case, all capacitance terms may be

$$\left(\frac{C_1}{\Delta T} + \frac{1}{R_1} \right) \theta_{i,1}^{m+1} - \frac{1}{R_1} \theta_{i,2}^{m+1} = Q_1 + \frac{C_1}{\Delta T} \theta_{i,1}^{m} \tag{17}$$

$$-\frac{1}{R_1} \theta_{i,1}^{m+1} + \left(\frac{1}{R_1} + \frac{1}{R_2} + \frac{C_2}{\Delta T} \right) \theta_{i,2}^{m+1} - \frac{1}{R_2} \theta_{i,3}^{m+1} = Q_2 + \frac{C_2}{\Delta T} \theta_{i,2}^{m} \tag{18}$$

$$-\frac{1}{R_2} \theta_{i,2}^{m+1} + \left(\frac{1}{R_2} + \frac{1}{R_3} + \frac{C_3}{\Delta T} \right) \theta_{i,3}^{m+1} - \frac{1}{R_4} \theta_{i,4}^{m+1} = Q_3 + \frac{C_3}{\Delta T} \theta_{i,3}^{m} \tag{19}$$

$$-\frac{1}{R_3} \theta_{i,3}^{m+1} + \left(\frac{1}{R_3} + \frac{1}{R_4} + \frac{C_4}{\Delta T} \right) \theta_{i,4}^{m+1} - \frac{1}{R_4} \theta_{i,5}^{m+1} = \frac{C_4}{\Delta T} \theta_{i,4}^{m} \tag{20}$$

$$-\frac{1}{R_4} \theta_{i,4}^{m+1} + \left(\frac{1}{R_4} + \frac{1}{R_5} + \frac{1}{Rr} \right) \theta_{i,5(c)}^{m+1} = \frac{1}{R_5} \theta_{i,6}^{m} + \frac{1}{Rr} \theta_{i,7}^{m} + Q_{5,y} \tag{21}$$

$$\left(\frac{1}{R_f}+\frac{1}{R_6}+\frac{C_6}{\Delta T}\right)\theta_{i,6}^{m+1}-\frac{1}{R_6}\theta_{i,7}^{m+1}=\sum_{c=1}^{N}\left(\frac{\left(\theta_{i,5(c)}^{m+1}-\theta_{i,6}^{m}\right)}{R_{5(c)}}\right)+\frac{1}{R_f}\theta_{i-1,6}^{m+1}+\frac{C_6}{\Delta T}\theta_{i,6}^{m} \quad (22)$$

$$-\frac{1}{R_6}\theta_{i,6}^{m+1}+\left(\frac{1}{R_6}+\frac{1}{R_7}+\sum_{c=1}^{N}\frac{1}{Rr(c)}\right)\theta_{i,7}^{m+1}-\frac{1}{R_7}\theta_{i,8}^{m+1}=\sum_{c=1}^{N}\frac{1}{Rr(c)}\theta_{i,5(c)}^{m+1} \quad (23)$$

$$-\frac{1}{R_{j-1}}\theta_{i,j-1}^{m+1}+\left(\frac{1}{R_{j-1}}+\frac{1}{R_j}+\frac{C_j}{\Delta T}\right)\theta_{i,j}^{m+1}-\frac{1}{R_j}\theta_{i,j+1}^{m+1}=\frac{C_j}{\Delta T}\theta_{i,j}^{m} \quad \text{j=8:n+6} \quad (24)$$

$$-\frac{1}{R_{n+7}}\theta_{i,n+6}^{m+1}+\frac{1}{R_{n+7}}\theta_{i,n+7}^{m+1}=0 \quad (25)$$

set to zero. The solution process can then be allowed to continue iterating until a desired level of convergence is reached. For most tunnel configurations this should require less than 20 iterations of the solution for the full length of the tunnel.

Transient

For transient calculations, it is necessary to define a suitable timestep such that calculation of the temperature distribution is accurate while simultaneously requiring the minimum possible number of iterations. In order to further enhance the transient solution, it is recommended that a temperature dependant a.c. resistance is introduced. This is easily achieved by replacing (7) and (9) with a function which is called prior to each solution of the cable system equations. The initial conditions within the transient calculation may also be defined as the temperature profile gained from a steady state calculation.

BENCHMARKS

In order to validate the performance of the new method, a series of comparisons have been undertaken against the original Electra 143 method. The cable geometries and heat transfer data used in this process are those published in [9]. The tunnel in this case is circular, with a diameter of 3m and a length of 1km. For the initial comparisons, one 3 phase 400kV cable circuit is modelled.

Steady State The simplest benchmark test entails setting the radiation view factors in the new method equal to those in Electra 143 (F_{cw}=0.9 and F_{cc}=0). The tunnel air inlet temperature is set to 20°C, with a steady state current of 2000A per phase. The results are compared for tunnel air velocities of 2, 3, 4 and 5m/s and are detailed in Tables I (Electra 143) and II (new method). Comparing the data in these tables shows agreement to within 2 decimal places between both methods.

TABLE I – Steady state results from Electra 143

Air Velocity / Temperature	2m/s	3m/s	4m/s	5m/s
Conductor (°C)	72.41	66.64	63.53	61.54
Cable Surface (°C)	41.87	36.10	32.98	31.00
Tunnel Air (°C)	32.09	28.06	26.05	24.84
Tunnel Wall (°C)	33.23	28.73	26.50	25.17

TABLE II – Steady state results from new method

Air Velocity / Temperature	2m/s	3m/s	4m/s	5m/s
Conductor (°C)	72.41	66.64	63.53	61.54
Cable Surface (°C)	41.86	36.09	32.98	30.99
Tunnel Air (°C)	32.09	28.06	26.05	24.84
Tunnel Wall (°C)	33.23	28.73	26.50	25.17

TABLE III – Steady state results with full radiation treatment

Air Velocity / Temperature	2m/s	3m/s	4m/s	5m/s
Conductor (°C)	72.35	66.60	63.49	61.54
Cable Surface (°C)	41.81	36.66	32.94	30.97
Tunnel Air (°C)	32.09	28.06	26.05	24.84
Tunnel Wall (°C)	33.27	28.75	26.52	25.19

The results shown in Table III are for the full method described within this paper (i.e. both F_{cw} and F_{cc} are calculated in full). The increased accuracy of viewfactor computation accounts for the slight change in values. From these results it is clear that the new steady state method performs well against the existing test case.

Transient To benchmark the transient method against Electra 143, both are solved for the case of a step application of a 2000A current for 24 hours. The initial conditions are a uniform temperature of 20°C, with an air inlet temperature of 20°C. The results are

TABLE IV – Transient results from Electra 143

Air Velocity / Temperature	2m/s	3m/s	4m/s	5m/s
Conductor (°C)	65.03	62.60	60.97	59.78
Cable Surface (°C)	34.64	32.16	30.50	29.29
Tunnel Air (°C)	25.59	24.53	23.82	23.31
Tunnel Wall (°C)	23.65	23.26	22.92	22.64

TABLE V – Transient results from new method

Air Velocity / Temperature	2m/s	3m/s	4m/s	5m/s
Conductor (°C)	65.00	62.57	60.95	59.76
Cable Surface (°C)	34.61	32.14	30.49	29.28
Tunnel Air (°C)	25.57	24.52	23.81	23.30
Tunnel Wall (°C)	23.63	23.24	22.91	22.63

TABLE VI – Transient results from new method (variable ac resistance and full radiation treatment)

Air Velocity / Temperature	2m/s	3m/s	4m/s	5m/s
Conductor (°C)	62.15	59.63	57.96	56.74
Cable Surface (°C)	33.06	31.31	29.74	28.60
Tunnel Air (°C)	25.18	24.19	23.53	23.05
Tunnel Wall (°C)	23.39	23.02	22.70	22.43

compared for tunnel air velocities of 2m/s to 5m/s and are detailed in Tables IV (Electra 143) and V (new method where F_{cw}=0.9). Comparing the data in these tables shows agreement to less than 0.05°C between both methods. These results validate the use of the new technique described here in calculating transient temperature distributions within cable tunnels. Where a variable a.c. resistance is incorporated into the new method, along with the full treatment of radiation heat exchange, the temperatures obtained are those in Table VI. It can be noted that the use of the variable resistance reduces conductor temperatures compared to the constant a.c. resistance, which over-estimates current dependent losses at lower temperatures.

CALCULATION OF RATINGS

Having established a reliable method for calculating temperature distributions within cable tunnels, it is possible to calculate circuit ratings for the case of independent cable circuits. In calculating current ratings for multiple cable circuits, a degree of insight into the operational constraints on each circuit is required in order to calculate a useful rating. For instance, it may be required to prioritise the steady state rating of one circuit over another where one cable is anticipated to feed an area of higher load demand.

To illustrate the flexibility of the new method, a 3m diameter 1km long deep tunnel is modelled as containing two independent 400kV cable circuits of the

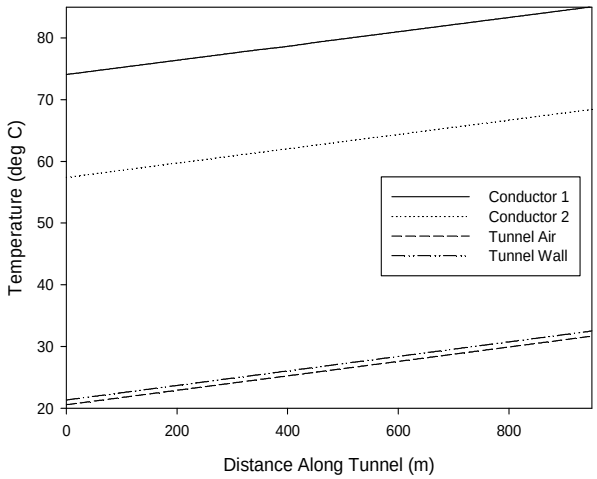

Figure 3 – Temperature profile for steady state rating calculation

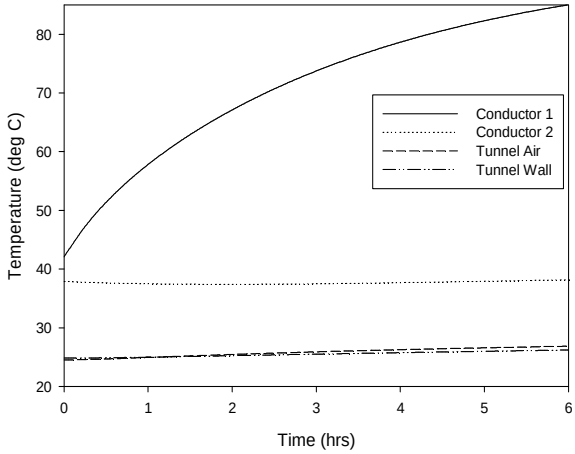

Figure 4 – Temperature Profile for 6hr emergency rating calculation

type described in [9]. The circuits are mounted on brackets on the tunnel wall and are cooled by forced air ventilation at a bulk flow rate of 5m/s, with a 20°C inlet temperature. One of the circuits can be assumed to require a maximum steady state power flow of 2000A. The current of the second circuit is then iterated to find the maximum steady state current through the second circuit. Assuming a conductor temperature limit of 85°C, the steady state rating of the second circuit is determined to be 2479A. The temperature of the air at the tunnel outlet is found to be 31.7°C. The temperature profiles are shown below in Fig. 3.

The steady state solution can be used to calculate initial conditions for emergency ratings. Assuming a 50% preload on both circuits, the 6 hour emergency rating is calculated for both circuits. This is achieved by calculating the steady state temperatures for currents corresponding to 50% of the steady state rating for each cable. The preload solution of the temperature distribution can then be used as the initial conditions in the transient calculation, with the current of the cable in question being increased iteratively until the

maximum conductor temperature criterion is reached. This analysis yields a 6 hour emergency rating for one circuit of 2750A, with the second circuit maintaining a steady current of 1000A. The temperature profile of the two circuits over the period of overload is shown in Fig. 4.

CONCLUSIONS

A new calculation method has been described for determining both the steady state and transient temperature distributions of cables installed within tunnels. Beneficial features of the present standard method of Electra 143 have been retained, but the requirement for all cables within the tunnel to be of identical construction and to carry identical load has been removed. The new method thus allows the solution of cable ratings where a number of independent cable circuits of different constructions and operating voltages may are installed in the same tunnel. Implementation of a variable a.c. resistance and the full calculation of radiation viewfactors increases the precision of the rating calculation. The extra flexibility within the new method allows more detailed ratings studies to be undertaken, hence making the best use of cable assets installed within tunnels.

Acknowledgement
The financial support of National Grid for this work is gratefully acknowledged.

References

1 *Haswell, C. K., "Thames cable tunnel" Proceedings of the Institution of Civil Engineers, Vol. 54 No. 1, pp451-486 (1970).*
2 *Sutton, S., Plath, R. and Schroder, G., "The St Johns Wood – Elstree Experience – testing a 20km long 400kV XLPE insulated cable system after installation" In Jicable '07, Versailles, France, 2007.*
3 *Knights, M., Mathews, J. and Marshall, B., "Revealed: London's network of power tunnels" Proceedings of ICE Civil Engineering, Vol. 144 No. 3, pp121-127 (2001).*
4 *Cigré, "Calculation of temperatures in ventilated cable tunnels" Electra, Vol. 143, pp 38-59 (1992).*
5 *Weedy, B. M. and El-Zayyat, H. M., "Heat transfer from cables in tunnels and shafts" IEEE Conf. Paper C72 506-4 (1972).*
6 *Long, C. A. "Essential Heat Transfer", Longman (1999).*
7 *Gray, W. A. and Muller, R. "Engineering calculations in radiative heat transfer" Permagon Press (1974).*
8 *Sparrow, E. M. and Cess, R. D. "Radiation heat transfer" Wadsworth Publishing (1966).*
9 *Cigré, "Calculation of temperatures in ventilated cable tunnels" Electra, Vol. 144, pp 97-105 (1992).*

LIST OF SYMBOLS

A_c	Conductor cross-sectional area (m^2)
A_f	Tunnel cross-sectional area (m^2)
C_j	Thermal capacitance at radial node j (J/K)
C_d	Capacitance of dielectric (F/m)
c_{pc}	Conductor specific heat capacity per unit volume (J/m^3K)
c_{pf}	Air specific heat capacity per unit volume (J/m^3K)
c_{pm}	Sheath specific heat capacity per unit volume (J/m^3K)
c_{ps}	Serving specific heat capacity per unit volume (J/m^3K)
c_{pt}	Dielectric specific heat capacity per unit volume (J/m^3K)
D_e	Outer cable diameter (m)
D_s	Cable sheath diameter (m)
D_{tun}	Tunnel diameter (m)
d_c	Conductor diameter (m)
F_{cc}	View factors between cables
F_{cw}	Radiation view factor from cable to wall
f	Frequency (Hz)
h_{cab}	Cable convective heat transfer coefficient (W/m^2K)
h_{wall}	Tunnel wall convective heat transfer coefficient (W/m^2K)
I	Phase current (A)
m	Time step identifier
N	Number of cables
n	Number of nodes in soil region
Q_j	Heat source at radial node j (W)
R_j	Thermal resistance between radial nodes j and j+1 ($K.m^2/W$)
R_{ac}	Conductor a.c. resistance (Ω/m)
t_1	Thickness of dielectric (m)
tanδ	Tangent of dielectric loss angle
U	Phase voltage (V)
V	Bulk air velocity (m/s)
ε_{cab}	Radiative emissivity of cable surface
$\theta_{i,j}$	Nodal temperature at axial location i, radial location j (°C)
λ	Sheath loss coefficient
ρ_s	Thermal resistivity of serving (K.m/W)
ρ_t	Thermal resistivity of dielectric (K.m/W)
σ	Stefan-Boltzmann constant
ΔT	Timestep used in transient calculation (s)
Δx	Axial slice separation (m)